Metal–Metal Bonding

DOI: 10.1002/anie.200601926

A Zinc–Zinc-Bonded Compound and Its Derivatives Bridged by One or Two Hydrogen Atoms: A New Type of Zn–Zn Bonding**

*Zhongliang Zhu, Robert J. Wright, Marilyn M. Olmstead, Eric Rivard, Marcin Brynda, and Philip P. Power**

Recently, the synthesis and structural characterization of decamethyldizincocene [Cp*ZnZnCp*] (**1**; Cp* = η^5-C_5Me_5, Zn–Zn 2.305(3) Å) was reported by Carmona and co-workers.[1] It was the first stable compound that contained a Zn–Zn bond.[2] This landmark development was confirmed by calculations which showed that the Zn–Zn bond is formed mainly by the overlap of the Zn 4s orbitals while the Zn 4p orbitals interact with the η^5-C_5Me_5 ligand.[1b,3] A further example of a compound with a Zn–Zn bond, [{HC(CMeNAr)$_2$}ZnZn{HC(CMeNAr)$_2$}] (Ar = 2,6-*i*Pr$_2$C$_6$H$_3$) (**2**), was reported by Robinson and co-workers,[4] and this species has a Zn–Zn bond length of 2.3586(7) Å. The zinc atoms are three-coordinate, and the metal–metal bond has 95% s character. The Zn–Zn bond in **2** is about 0.05 Å longer than that in **1** despite its lower metal coordination number. Clearly, the type of ligand exerts a large influence on the Zn–Zn bond length. It is therefore desirable to have zinc–zinc-bonded species in which the Zn atoms are bound to only one ligand atom to provide the simplest possible bonding arrangement and also to show that Zn–Zn bonds can in fact be stabilized by monodentate ligands. Furthermore, the synthesis of the singly or doubly bridged hydride derivatives of such a species would provide further information on the nature of the Zn–Zn bonding. We now describe the synthesis and characterization of the zinc–zinc-bonded species Ar′ZnZnAr′ (**4**) (Ar′ = C_6H_3-2,6-(C_6H_3-2,6-*i*Pr$_2$)$_2$), the hydride-bridged dimer Ar′Zn(μ-H)$_2$ZnAr′ (**5**), which has a Zn···Zn separation very similar to that in **4**, and the unique compound Ar′Zn(μ-H)(μ-Na)ZnAr′ (**6**), in which the Zn atoms are connected by a new type of Zn–Zn interaction.

Dinuclear **4** was synthesized by the reduction of Ar′ZnI (**3**) with Na. The hydride, Ar′Zn(μ-H)$_2$ZnAr′ (**5**), was prepared by the treatment of **3** with NaH. Rather than forming zinc–zinc-bonded compound **4** (as indicated in the indirect route for **1** whereby KH was used to reduce the [Zn(Cp*)$_2$] species in situ[1b] or whereby [Cp*ZnZnCp*] was obtained by the unforeseen ligand exchange between [ZnCp*$_2$] and ZnEt$_2$[1a] (Scheme 1)), further reduction of **5** by NaH provided the unprecedented sodium hydride-bridged species Ar′Zn(μ-H)(μ-Na)ZnAr′ (**6**, Scheme 2).

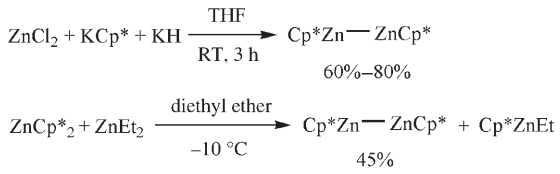

Scheme 1. Synthetic routes to the zinc–zinc-bonded dimer [Cp*ZnZnCp*] (**1**).[1]

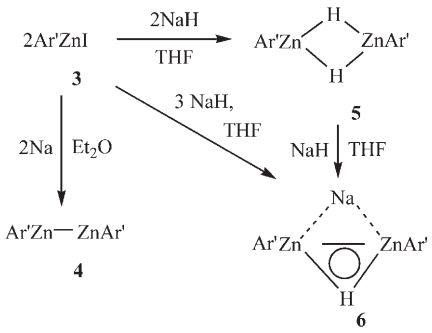

Scheme 2. Synthetic routes to **4**, **5**, and **6**.

The crystal structure of **4** (Figure 1)[5] confirms the presence of a Zn–Zn bond. The observed Zn–Zn bond length in **4** (2.3591(9) Å) is about 0.05 Å larger than that in **1** (2.305(3) Å) and is essentially the same as that in **2** (2.3586(7) Å). The two Ar′ ligands are arranged in a nearly orthogonal orientation to each other, which provides effective steric protection of the Zn–Zn moiety. An almost linear arrangement is observed for the {C(*ipso*)-Zn-Zn-C(*ipso*)} interior, which is in contrast to the other known metal–metal-bonded dimers ArMMAr, (M = Cr,[6a] Ga,[6b] Ge,[6c] As,[6d] or Se[6e]) which for numerous reasons display strongly *trans*-bent geometries.

[*] Z. Zhu, Dr. R. J. Wright, Prof. M. M. Olmstead, Dr. E. Rivard, Dr. M. Brynda, Prof. P. P. Power
Department of Chemistry
University of California
One Shields Avenue, Davis, CA 95616 (USA)
Fax: (+1) 530-752-8995
E-mail: pppower@ucdavis.edu

[**] The authors thank the National Science Foundation for financial support. E.R. thanks NSERC of Canada for a postdoctoral fellowship.

Supporting information for this article is available on the WWW under http://www.angewandte.org or from the author.

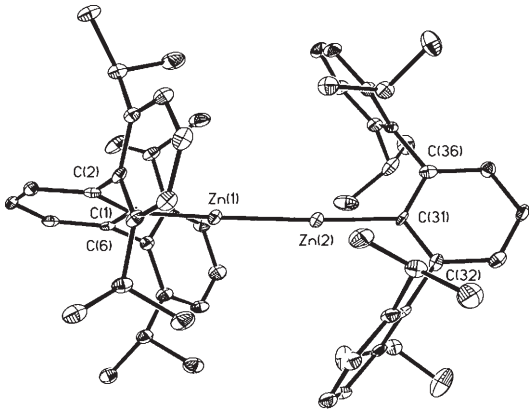

Figure 1. Thermal-ellipsoid plot (ellipsoids set at 30% probability) of **4** without hydrogen atoms. Selected bond lengths [Å] and angles [°]: Zn(1)-Zn(2) 2.3591(9), Zn(1)-C(1) 1.965(6), Zn(2)-C(31) 1.974(5); C(31)-Zn(2)-Zn(1) 177.28(18), Zn(2)-Zn(1)-C(1) 177.57(18), C(32)-C(31)-Zn(2) 120.5(4), C(36)-C(31)-Zn(2) 119.1(4).

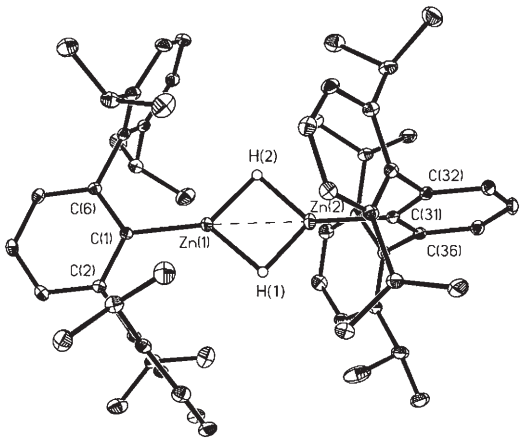

Figure 2. Thermal-ellipsoid plot (ellipsoids set at 30% probability) of **5** without hydrogen atoms. Selected bond lengths [Å] and angles [°]: Zn(1)···Zn(2) 2.4084(3), Zn(1)-H(1) 1.67(2), Zn(1)-H(2) 1.79(3), Zn(1)-C(1) 1.9301(16); C(1)-Zn(1)-Zn(2) 175.14(5), Zn(1)-Zn(2)-C(31) 175.60(5), C(1)-Zn(1)-H(1) 138.3(9), Zn(2)-Zn(1)-H(1) 45.2(8), C(6)-C(1)-Zn(1) 121.21(11), C(2)-C(1)-Zn(1) 120.00(12).

Well-characterized, stable Zn–H species are relatively rare because of the high tendency of these species to oligomerize or polymerize.[7] Nonetheless, the synthesis of **5**[5] proceeded smoothly and in moderate yield. The bridging hydrogen atoms in **5** were located in the electron difference map. The overall appearance of the molecular structure of **5** (Figure 2) and perpendicular orientation of the ligands are very similar to those of **4** (crystals of **4** and **5** are isomorphous), and the Zn···Zn separation in **5** (2.4084(3) Å) is lengthened by only about 0.05 Å in comparison with that in **4**. In the ^{1}H NMR spectrum a signal corresponding to the bridging hydride in **5** was located at $\delta = 4.84$ ppm, in a 1:1 intensity ratio with the signals of the aryl ligand. A similar chemical shift was observed at $\delta = 4.59$ ppm in the zinc hydride [RZn(μ-H)$_2$ZnR] (R = [{(2,6-*i*Pr$_2$C$_6$H$_3$)N(Me)C}$_2$-CH]; Zn···Zn 2.4513(9) Å).[7e] It is notable that the Zn···Zn separation in this hydride species is about 0.1 Å longer than that seen in the zinc–zinc-bonded β-diketiminate derivative **2**.[4]

DFT calculations[8,9] for **4** (Figure 3) were performed at the B3LYP/6-31g* level and indicate that the HOMO is localized mainly in the Zn–Zn σ-bonding region with some additional Zn–C(*ipso*) σ-bonding character. The LUMO and LUMO + 1 consist of two almost degenerate orbitals of π symmetry, which are localized mostly on the central {Zn–Zn}$^{2+}$ unit. These calculations show that the Zn–Zn bond is formed from the overlap of mainly 4p$_z$ orbitals in the HOMO, thus leaving two empty orthogonal p$_x$ and p$_y$ orbitals to form the π-symmetric LUMOs. The 4s orbitals of the zinc centers are mainly involved in bonding to the *ipso* carbon atoms of the ligands. In contrast to **4**, the Zn 4s orbitals form the Zn–Zn bond in **1**, and this Zn–Zn bonding orbital is the HOMO−4. The orbitals HOMO to HOMO−3 of **1** are mostly ligand-based π levels of the η^5-C$_5$Me$_5$ ring. In **2**, the Zn–Zn bond is the HOMO, and the LUMO is a ligand orbital of π symmetry.

The sodium hydride bridged compound **6**[5] could be obtained from **3** or **5** by the reaction with the appropriate number of equivalents of NaH (Scheme 2). The Zn–Zn bond length in **6** is 2.352(2) Å (Figure 4), which is essentially the same as that in **4** (2.3591(9) Å). In contrast to **4** and **5**, the two central aryl rings on the Ar′ ligand are nearly coplanar in **6**, and the bridging sodium and hydride centers also lie near this plane. The Na$^+$ counterion is sequestered by strong η^6 interactions involving the flanking aryl rings on the Ar′ ligand. The Na$^+$···C(aryl) separations range from 2.843 to 3.108 Å, and the Na$^+$–centroid distances of the two flanking aryl rings are 2.658 Å and 2.670 Å, respectively. In addition, the two sets of Zn···Na$^+$ and Zn···H$^-$ distances are 3.113(4)/3.130(4) Å and 1.75(6)/1.74(6) Å, respectively. The ^{1}H NMR spectrum of **6** displays a broad signal at $\delta =$ 2.04 ppm, which was assigned to the bridging hydride.

The metal–metal bonding in **6** differs considerably from that observed in **4**. The DFT calculations indicate that there is a delocalized orbital formed by the bridging hydrogen atom and two zinc atoms, as illustrated in HOMO−17 (Figure 5). In contrast to **4**, 4s orbitals of zinc atoms participate in the

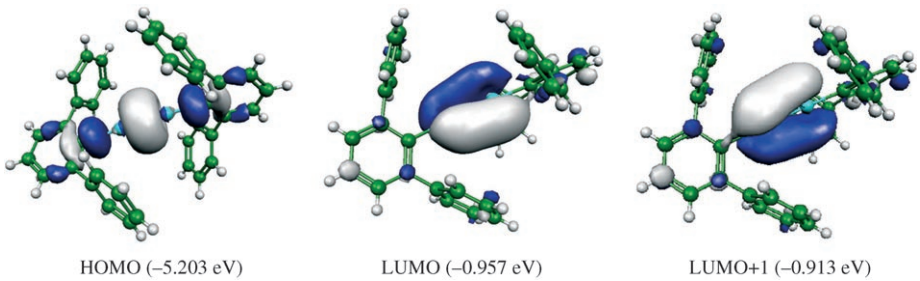

Figure 3. Representation of the key molecular orbitals of **4** from DFT calculations.

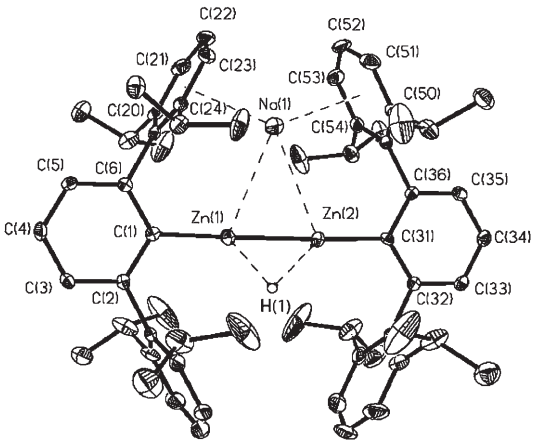

Figure 4. Thermal-ellipsoid plot (ellipsoids set at 30% probability) of **6** without hydrogen atoms. Selected bond lengths [Å] and angles [°]: Zn(1)-Zn(2) 2.352(2), Zn(1)-H(1) 1.75(6), Zn(1)-Na(1) 3.113(4), Zn(1)-C(1) 1.977(5); C(1)-Zn(1)-Zn(2) 170.38(15), Zn(2)-Zn(1)-Na(1) 68.25(5), Zn(2)-Zn(1)-H(1) 47.6(18), Zn(1)-Na(1)-Zn(2) 44.26(7), C(6)-C(1)-Zn(1) 121.21(11), C(2)-C(1)-Zn(1) 120.00(12); dihedral angles: between the C1–C6 and C31–C36 planes 1.9°, between the C1–C6 and Zn_2HNa planes 8.9°, between the C31–C36 and Zn_2HNa planes 9.3°.

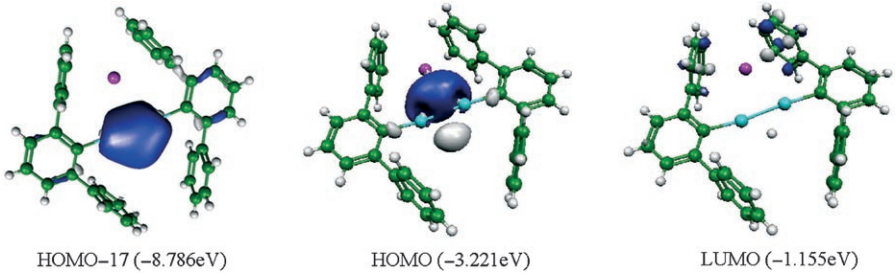

Figure 5. Representation of the key molecular orbitals of **6** from DFT calculations.

HOMO−17 bonding interaction to yield an orbital that has both Zn−Zn and Zn−H bonding character. The HOMO of **6** has considerable electron density in the region between the Na^+ ion and the zinc atoms, and between the zinc centers. There is also a smaller region of electron density of opposite phase near the bridging hydrogen atom such that the orbital resembles a distorted Zn−Zn bonding interaction of π symmetry. However, the Wiberg bond order[9] calculations indicate that the Zn−Zn bond order (0.81) in **6** is slightly less than that (0.95) in **4** with a considerable bonding interaction between the zinc centers and sodium atom (bond order 0.68).

In conclusion, a new zinc–zinc-bonded compound supported by monodentate ligands has been synthesized by a straightforward procedure. The related hydrogen-bridged dimer shows that, although it has no Zn−Zn bond, the metal–metal separation is only about 0.05 Å longer. In contrast to the zinc–zinc-bonded compounds **1** and **2**,[1,4] the Zn−Zn bond in Ar′ZnZnAr′ (**4**) is formed by using mainly $4p_z$ orbitals. DFT calculations and the structure parameters indicate a new type of Zn−Zn bond in **6**. Future work will focus on investigations of the reactivity of the Zn−Zn bond in compounds **4**, **6**, and related species.

Experimental Section

All manipulations were carried out under anaerobic and anhydrous conditions. ^1H and ^{13}C NMR spectra were recorded on a Varian 300 spectrometer and referenced to known standards.

4: A solution of **3** (0.93 g, 1.58 mmol) in diethyl ether (50 mL) was added to a Schlenk tube containing finely cut Na (0.036 g, 1.58 mmol) at about 25 °C. After stirring for 2 days, some Zn metal was precipitated. The solution was filtered, and the solvent was removed in a dynamic vacuum. The residue was redissolved in hexane (5 mL), and storage for 2 days in a freezer (ca. −40 °C) afforded large colorless X-ray quality crystals of **4**. Yield: 0.174 g, 23.9%; m.p. > 360 °C (when the temperature was kept at ca. 360 °C for several minutes, **4** decomposed, and a black solid was deposited); ^1H NMR (300 MHz, C_6D_6, 25 °C): $\delta = 1.00$ (d, 12H, *o*-CH(CH_3)$_2$, $^3J_{HH} = 6.9$ Hz), 1.12 (d, 12H, *o*-CH(CH_3)$_2$, $^3J_{HH} = 6.9$ Hz), 2.86 (sept, 4H, $CH(CH_3)_2$, $^3J_{HH} = 6.9$ Hz), 7.06–7.24 ppm (m, 9H, *m*-C_6H_3, *p*-C_6H_3, *m*-Dipp, and *p*-Dipp; Dipp = 2,6-*i*$Pr_2C_5H_3$); $^{13}C\{^1H\}$ NMR (C_6D_6, 100.6 MHz, 25 °C): $\delta = 24.7$ ($CH(CH_3)_2$), 24.8 ($CH(CH_3)_2$), 30.4 ($CH(CH_3)_2$), 123.0 (*m*-Dipp), 125.7 (*p*-C_6H_3), 127.6 (*p*-Dipp), 128.3 (*m*-C_6H_3), 142.3 (*i*-Dipp), 146.9 (*o*-C_6H_3), 147.4 (*o*-Dipp), 162.4 ppm (*i*-C_6H_3).

5: The iodide derivative **3** (1.00 g, 1.70 mmol) and NaH (0.060 g, 2.50 mmol) were combined with THF (50 mL) under an inert atmosphere of dry argon at ambient temperature. The mixture was stirred for 2 days, the solvent was then removed in a dynamic vacuum, and the residue was extracted with hexane (50 mL). The slurry was allowed to settle, and the mother liquor was separated from the precipitate (NaI and excess NaH). The volume was concentrated to about 10 mL, and storage for 2 days in a freezer (ca. −40 °C) afforded colorless X-ray quality crystals of **5**. Yield: 0.81 g, 89.1% (based on **3**); decomposed before melting (loss of crystallinity started at 210 °C, and decomposition of **5** to a black solid was observed at 290°); ^1H NMR (300 MHz, C_6D_6, 25 °C): $\delta = 1.01$ (d, 12H, *o*-CH(CH_3)$_2$, $^3J_{HH} = 6.9$ Hz), 1.11 (d, 12H, *o*-CH(CH_3)$_2$, $^3J_{HH} = 6.9$ Hz), 2.91 (sept, 4H, $CH(CH_3)_2$, $^3J_{HH} = 6.9$ Hz), 4.84 (s, 1H, ZnH), 7.04–7.25 ppm (m, 9H, *m*-C_6H_3, *p*-C_6H_3, *m*-Dipp, and *p*-Dipp); $^{13}C\{^1H\}$ NMR (C_6D_6, 100.6 MHz, 25 °C): $\delta = 24.3$ ($CH(CH_3)_2$), 25.1 ($CH(CH_3)_2$), 30.6 ($CH(CH_3)_2$), 123.2 (*m*-Dipp), 126.0 (*p*-C_6H_3), 127.8 (*p*-Dipp), 128.5 (*m*-C_6H_3), 143.4 (*i*-Dipp), 146.7 (*o*-C_6H_3), 148.7 (*o*-Dipp), 155.7 ppm (*i*-C_6H_3); IR (nujol): $\tilde{\nu}_{(Zn\text{-}H)}$ bands are likely obscured by overlapping of ligand vibrations.

6: Compound **5** (0.50 g, 1.08 mmol) and NaH (0.039 g, 1.62 mmol) were combined in THF (50 mL). The mixture was stirred for 2 days, the solvent was then removed in a dynamic vacuum, and the residue was extracted with PhMe (50 mL). The slurry was allowed to settle, and the mother liquor was separated from the precipitate (NaH) by a filter cannula. The solvent volume was concentrated to about 10 mL, and storage for 2 days in a freezer (ca. −18 °C) afforded colorless X-ray quality crystals of **6**. Yield: 1.03 g, 87.3% (based on **5**); decomposed before melting (loss of crystallinity started at 235 °C, and decomposition of **6** to a black solid was seen at 268 °C); ^1H NMR (300 MHz, C_6D_6, 25 °C): $\delta = 1.09$ (d, 12H, *o*-CH(CH_3)$_2$, $^3J_{HH} = 6.9$ Hz), 1.15 (d, 12H, *o*-CH(CH_3)$_2$, $^3J_{HH} = 6.9$ Hz), 2.04 (br, 1H, Zn_2NaH), 2.99 (sept, 4H, $CH(CH_3)_2$, $^3J_{HH} = 6.6$ Hz), 7.01–7.27 ppm (m, 9H, *m*-C_6H_3, *p*-C_6H_3, *m*-Dipp, and *p*-Dipp); $^{13}C\{^1H\}$ NMR (C_6D_6, 100.6 MHz, 25 °C): $\delta = 23.6$ ($CH(CH_3)_2$), 25.2 ($CH(CH_3)_2$), 30.7 ($CH(CH_3)_2$), 122.4 (*m*-Dipp), 127.3 (*p*-C_6H_3), 146.8 (*i*-Dipp), 148.1 (*o*-C_6H_3), 148.8 (*o*-Dipp), 158.7 ppm (*i*-C_6H_3), *m*-C_6H_3 and *p*-Dipp

resonances are likely obscured by the C_6H_6 signal; IR (nujol): $\tilde{\nu}_{(Zn\text{-}H)}$ bands are likely obscured by overlapping of ligand vibrations.

Received: May 16, 2006
Published online: August 14, 2006

Keywords: density functional calculations · hydride ligands · steric hindrance · structure elucidation · zinc

[1] a) I. Resa, E. Carmona, E. Gutierrez-Puebla, A. Monge, *Science* **2004**, *305*, 1136 – 1138; b) D. del Río, A. Galindo, I. Resa, E. Carmona, *Angew. Chem.* **2005**, *117*, 1270 – 1273; *Angew. Chem. Int. Ed.* **2005**, *44*, 1244 – 1247.

[2] Some examples of Hg–Hg bonds and Cd–Cd bonds have been reported: a) D. Brwvo-Zhivotovskii, M. Yozefovich, M. Bendikov, Y. Apeloig, *Angew. Chem.* **1999**, *111*, 1169 – 1171; *Angew. Chem. Int. Ed.* **1999**, *38*, 1100 – 110; b) R. Faggiani, R. J. Gillespie, J. E. Vekris, *J. Chem. Soc. Chem. Commun.* **1986**, 517; c) D. L. Reger, S. S. Mason, A. L. Rheingold, *J. Am. Chem. Soc.* **1993**, *115*, 10406 – 10407.

[3] a) Y. Xie, H. F. Schaefer III, R. B. King, *J. Am. Chem. Soc.* **2005**, *127*, 2818 – 2819; b) H. S. Kang, *J. Phys. Chem. A* **2005**, *109*, 4342 – 4351; c) J. W. Kress, *J. Phys. Chem. A* **2005**, *109*, 7757 – 7763; d) Z.-Z. Xie, W. H. Fang, *Chem. Phys. Lett.* **2005**, *404*, 212 – 216; e) Z.-Z. Liu, W. Q. Tian, J.-K. Feng, G. Zhang, W.-Q. Li, *J. Mol. Struct.* **2006**, *758*, 127 – 138.

[4] Y. Wang, B. Quillian, P. Wei, H. Wang, X.-J. Yang, Y. Xie, R. B. King, P. von R. Schleyer, H. F. Schaefer III, G. H. Robinson, *J. Am. Chem. Soc.* **2005**, *127*, 11944 – 11945.

[5] Crystallographic data for **4**, **5**, and **6** were recorded at 90 K with $Mo_{K\alpha}$ radiation ($\lambda = 0.71073$ Å). **4**: $a = 12.2630(15)$, $b = 16.883(2)$, $c = 12.6996(16)$ Å, $\beta = 92.419(2)°$, monoclinic, space group $P2_1$, $Z = 2$, $R1 = 0.0650$ for 9529 ($I > 2\sigma(I)$) data, w$R2$ (all data) = 0.1481. **5**: $a = 12.3101(8)$, $b = 16.8622(10)$, $c = 12.6693(8)$ Å, $\beta = 92.9500(10)°$, monoclinic, space group $P2_1$, $Z = 2$, $R1 = 0.0316$ for 15989 ($I > 2\sigma(I)$) data, w$R2$ (all data) = 0.0722. **6**: $a = 16.641(17)$, $b = 16.656(17)$, $c = 28.38(3)$ Å, $\beta = 109.722(19)°$, monoclinic, space group $P2_1/c$, $Z = 4$, $R1 = 0.0642$ for 10647 ($I > 2\sigma(I)$) data, w$R2$ (all data) = 0.1557. CCDC-606921 (**4**), CCDC-606920 (**5**), and CCDC-606922 (**6**) contain the supplementary crystallographic data for this paper. These data can be obtained free of charge from The Cambridge Crystallographic Data Centre via www.ccdc.cam.ac.uk/data_request/cif.

[6] a) T. Nguyen, A. D. Sutton, M. Brynda, J. C. Fettinger, G. J. Long, P. P. Power, *Science* **2005**, *310*, 844 – 847; b) N. J. Hardman, R. J. Wright, A. D. Phillips, P. P. Power, *J. Am. Chem. Soc.* **2003**, *125*, 2667 – 2679; c) M. Stender, A. D. Phillips, R. J. Wright, P. P. Power, *Angew. Chem.* **2002**, *114*, 1863 – 1865; *Angew. Chem. Int. Ed.* **2002**, *41*, 1785 – 1787; d) B. Twamley, C. D. Sofield, M. M. Olmstead, P. P. Power, *J. Am. Chem. Soc.* **1999**, *121*, 3357 – 3367; e) J. J. Ellison, K. Ruhlandt-Senge, H. H. Hope, P. P. Power, *Inorg. Chem.* **1995**, *34*, 49 – 54.

[7] a) N. A. Bell, P. T. Moseley, H. M. M. Shearer, C. B. Spencer, *J. Chem. Soc. Chem. Commun.* **1980**, 359; b) A. Looney, R. Han, I. B. Gorrell, M. Cornebise, K. Yoon, G. Parkin, A. L. Rheingold, *Organometallics* **1995**, *14*, 274 – 284; c) W. Kläui, U. Schilde, M. Schmidt, *Inorg. Chem.* **1997**, *36*, 1598; d) M. Krieger, B. Neumüller, K. Dehnicke, *Z. Anorg. Allg. Chem.* **1998**, *624*, 1563; e) H. Hao, C. Cui, H. W. Roesky, G. Bai, H.-G. Schmidt, M. Noltemeyer, *Chem. Commun.* **2001**, 1118 – 1119.

[8] F. Weinhold, C. R. Landis, *Valency and Bonding. A Natural Bond Orbital Donor-Acceptor Perspective*, Cambridge University Press, Cambridge, **2005**, p. 556.

[9] DFT calculations were performed at the B3LYP/6-31g* level by using simplified models based on the X-ray diffraction structures of **4** and **6** on which isopropyl groups of the flanking aryls were replaced with protons. The single point (SP) calculations were performed by using Gaussian 03 software (Gaussian 03 (Revision B.03): M. J. Frisch et al. (see the Supporting Information). The representations of Kohn–Sham orbitals were generated using the MOLEKEL package (MOLEKEL, P. Flukiger, H. P. Luthi, S. Portmann, J. Weber, MOLEKEL 4.3, Swiss Center for Scientific Computing, Manno, Switzerland, **2000–2002**), and the Wiberg bond orders were computed from SP B3LYP/6-31g* calculations using the AOMix program (AOMIX, S. I. Gorelsky, AOMix program, Rev. 5.44, http://www.obbligato.com/software/aomix/).

